Research Article

Polyaniline-coated *Calotropis procera* L. hollow tubular fibers with remarkable antibacterial activity

Marcelo Reis dos Santos[1] · Fernando Antonio Gomes da Silva Jr.[1] · Poliana Pereira Ferrais[1] · Ricardo Santana de Lima[1] · Mateus Matiuzzi da Costa[1] · Helinando Pequeno de Oliveira[1]

Received: 27 March 2020 / Accepted: 16 August 2020 / Published online: 25 August 2020

Abstract
The development of environmentally friendly prototypes for use as antibacterial agents and as alternatives to antibiotics is a necessary step toward the control of infections. With this in mind, the production of hybrid composites based on natural and synthetic materials has been successfully explored. Herein, the chemical polymerization of polyaniline on natural fibers of *Calotropis procera* was used to explore the combined available surface area of fibers with the intrinsic properties of the conductive layer of PANI. What resulted was a coating of conducting polymer on natural fibers with strong antibacterial activity against *Staphylococcus aureus* and *Escherichia coli*. The characteristic time for the complete elimination of colonies (kill time) observed in assays was in the region of 3–4 h of treatment, with an inhibition halo of 20 mm (against *E. coli*) and 24 mm (against *S. aureus*). In addition to the antibacterial activity against *S. aureus* and *E. coli*, the modified fibers exhibited antibiofilm activity against *S. aureus*, which was evidenced in the reduction in the degree of bacterial adhesion to the surface applied in treatment (with a 39.96% biofilm inhibition). The proposed method represents a simple, low-cost, and one-step method for the modification of natural fibers with relevant applications in antibacterial agents.

Keywords Hollow fibers · *Calotropis procera* · Polyaniline · Antibacterial

1 Introduction

Resistance to antibiotics is one of the most serious healthcare problems, caused by the development of resistance mechanisms acquired by bacterial strains against several antibiotic classes [1]. These so-called superbugs have been critical not only in the hospital environment but also in the community. In addition, the scarcity of new effective antibiotics reinforces the need for strategies in the development of alternative antibacterial agents. In particular, the use of conducting polymers [2–4] as antibacterial agents has been considered a promising strategy. In general, the production of structures with large surface area and a well-defined morphology plays a critical role in the performance of hierarchical devices. This has required strategies that involve expensive chemicals. As an alternative, the guided growth of a conducting polymer layer on the surface of natural microtubes can allow for the exploitation of the intrinsic advantages of these materials.

Calotropis procera is a flowering plant that belongs to the family *Asclepedaceae* (genus *Calotropis*) [5–8], which originates from Africa, India, and Persia [9], and has adapted to tropical and subtropical lands with characteristic sandy soil and low rainfall. This plant is recognized as a source of medicinal products, derived from its essential oils, leaves, and bark [6, 9, 10], presenting anti-inflammatory, antibacterial, antioxidative, and antifungal properties [9, 11, 12]. In addition, digestive properties

✉ Helinando Pequeno de Oliveira, helinando.oliveira@univasf.edu.br | [1]Institute of Materials Science, Federal University of Sao Francisco Valley, Juazeiro, BA 48920-310, Brazil.

[13] have been attributed to its flowers. Pattnaik et al. [14] reported that these medicinal properties arise from phytochemical groups observed in leaf extracts of *C. procera*: fatty acid ethyl ester, palmitic acid ester, linoleic acid, and amino acids. It is worth mentioning that, to our knowledge, all of the antibacterial and medicinal activities of *C. procera* derivatives have been associated with ethanolic extracts from parts of the plants. No antibacterial activity has been attributed to *C. procera* fruit fibers, which are cellulose-based hollow tubes with a diameter of 30–50 µm and an open-ended structure with large lumens [15]. The characteristic hydrophobic–oleophilic surface of fibers offers conditions for oil-absorbing applications [16]. However, the applications are not restricted to adsorption, since *C. procera* fibers have been explored as a binding material for fabrics and as support for chemical modification in composites [17].

In particular, the waxy surface of *C. procera* could provide a conducive environment for the adhesion of the monomers and the subsequent step of guided polymerization. This process [15] has been developed for the production of composites that are applied in the environmental detection of micropollutants, such as fluoroquinolone-based antibiotics.

The coating of hollow tubes of *C. procera* with conducting polymers introduces desirable properties for various applications. However, to our knowledge, there is no publication that reports on the development of hybrid composites based on *C. procera* and polyaniline (PANI) with intrinsic antibacterial activity.

It has been reported that the antibacterial activity of PANI [18–21] involves the production of hydrogen peroxidase, which is favored by aerobic conditions, due to the conducive conditions for the generation of reactive oxygen species [22]. Hydroxyl compounds cause damage to cell walls, leading to eventual cell death. Dhivya et al. [23] reported that the doping level plays a critical role in antibacterial activity since the low antibacterial activity was reported for the emeraldine base. These results are in agreement with those reported by Kucekova et al. [24] and confirm that emeraldine salt introduces superior antibacterial activity in comparison with the corresponding base. Further combinations in composites with Cu, ZnO [25], and silver nanoparticles [24] have been explored to improve the antibacterial activity of the resulting material.

Herein, we propose a simplification of the chemical procedure for the production of new nanostructured antibacterial materials that are based on hollow microtubes, making use of natural material (specifically *C. procera* fibers) as a surface for modification, and a one-step synthesis procedure for the production of the polymeric film coating layer.

2 Material and methods

2.1 Materials

The fibers of *C. procera* were collected at Univasf, Juazeiro, Bahia, Brazil. Aniline (Sigma-Aldrich), ammonium persulfate (APS, Sigma-Aldrich), hydrochloric acid (Vetec), Mueller–Hinton Agar (Himedia), tryptic soy broth (TSB, Fluka), and plate counter agar (PCA) were used as received. Ultrapure water ($\rho = 18.2$ MΩ cm) was used in all the steps for sample preparation. Aniline was distilled before use. Gram-positive *S. aureus* (ATCC 25923) and Gram-negative *E. coli* (ATCC 25922) were used in the antibacterial assays. In particular, *S. aureus* and *E. coli* represent a group of pathogens with large concern about conventional antimicrobial drug resistance in hospitals and the community. The Mueller–Hinton assay (composed by a low nutrient content) simulates conditions such as surfaces and environment in which *S. aureus* and *E. coli* are more persistent to antimicrobial drugs, characterizing an important condition to evaluate the activity of the antibacterial agents. All of the experiments were performed in triplicate and negative controls returned no external contamination to affect the microbiology assays.

2.1.1 Preparation of PANI-coated *C. procera* (PANI-CP) hollow tubes

The synthesis of PANI followed the general steps described in Ref. [2] with some modifications: *C. procera* fibers were freshly washed with Milli-Q water and dried at 50 °C for 6 h. In the following step, 150 µL of aniline monomers was dissolved in hydrochloric acid (50 mL at 1.0 M). Fibers of *C. procera* (1 g) were then incorporated into the solution, which was kept under continuous stirring in an ice bath. A second solution was prepared using APS (125 mg) in 10 mL of an aqueous solution. This solution was then added dropwise into the first solution containing aniline and *C. procera*. The polymerization takes place with the resulting solution kept under stirring in an ice bath for 2 h. The resulting composite was washed with ultrapure water and then dried in an oven for 24 h at 50 °C. The standard chemical polymerization of polyaniline depends on the action of an oxidizing agent (ammonium persulfate) that interacts with aniline monomers in an acidic environment. The process of polymerization starts with the transfer of an electron from the nitrogen of aniline; the formed cation can be deprotonated or rearranged in a dimmer. Under acidic conditions, the interaction of head with

tail is favored, resulting in aggregation in the form of dimers. A new oxidative step takes place, allowing a new cation to be formed, which acquires a configuration of a trimer or tetramer. The sequence of steps continues until the complete polymerization of PANI is reached. In the absence of support, the polymerization process results in the formation of aggregates and grains of PANI. The introduction of templates into reactors induces a specific morphology for the material under polymerization. This process has been reported for the oriented growth of polypyrrole [26] or nanoparticles [27] on *Calotropis gigantea* fibers. The process of oriented growth of polymeric chains on natural fibers in response to their excellent hydrophobic–oleophilic properties is due to their characteristic wax coating layers. Consequently, the monomers are confined to the surface of dispersed hollow tubular structures that impose a spatial limitation for polymeric growth, which tends to cover the available surfaces [28].

The overall process of polymerization that provides the complete coating of tubes by a thin layer of PANI is summarized and schematically shown in Fig. 1.

As shown, the pristine fibers (white fibers) are completely coated by a thin layer of PANI (green fibers) after 2 h of reaction (in situ polymerization).

2.1.2 Antibacterial assays

The antibacterial activity of PANI-CP was evaluated according to standard assays of agar diffusion, kill time, and biofilm adhesion applied to *S. aureus* and *E. coli*. The agar diffusion tests follow a standard procedure described by CLSI 2019. An inoculum of both species was preserved in agar at 4 °C. Colonies of *S. aureus* and *E. coli* were dispersed in a Petri dish with Mueller–Hinton Agar at 10^8 CFU. Circular disks (1 cm) of *C. procera* (control experiment), PANI, and PANI-CP were pressed and placed on agar plates, which were incubated at 37 °C for 24 h.

The kill time assays were evaluated using *S. aureus* and *E. coli* (at a corresponding concentration of 0.5 at the McFarland scale). Aliquots of 1 mL of each bacterial solution were dispersed in 9 mL of the saline aqueous solution. Then, the samples *C. procera* (CP), PANI, and PANI-CP (10 mg) were immersed in a saline aqueous solution (*S. aureus* and *E. coli*) for 4 h. At a fixed interval of time (0.5, 1, 2, 3, and 4 h), aliquots of saline solution (100 µL) were inoculated into the Petri dishes for 24 h at 37 °C in triplicate to evaluate the total number of viable cells.

To identify the degree of biofilm inhibition on fibers, the first step concerns the preparation of a tryptic soy broth solution (TSB) with glucose (0.25% in weight), with 10^7 CFU mL^{-1} of corresponding bacteria under analysis

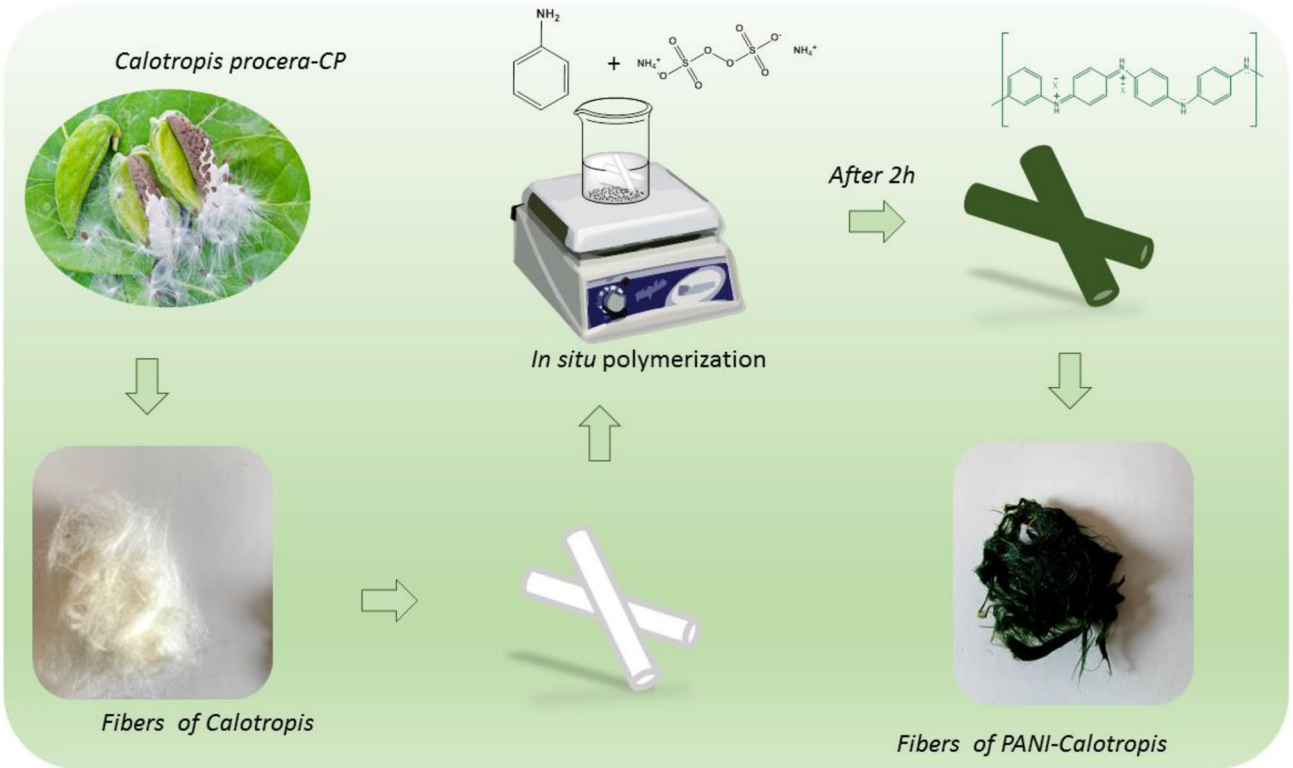

Fig. 1 Scheme of the complete process of separation of fibers and polymeric coating of PANI on *C. procera*

(*S. aureus* or *E. coli*) that incorporates *C. procera* and PANI-CP into reactors, with the solution incubated for 24 h at 37 °C. After this step, the fibers were removed from the reactor, washed with ultrapure water to remove unbound organisms, and then immersed in crystal violet (0.25% wt in water) for 5 min, with the excess dye removed by washing. The resulting samples were immersed in 10 mL of alcohol:acetone (80:20) mixture for the desorption of the dye from the fibers. The absorbance at 570 nm of resulting solution provides a direct measurement of biofilm formation on the fibers. The percentage of biofilm adhesion on the fibers is calculated as follows:

$$\%\text{Biofilm inhib}\,(\%\text{BI}) = 100 \times \left(\frac{A_{\text{CP}} - A_{\text{panicp}}}{A_{\text{CP}}}\right) \quad (1)$$

where A_{CP} is the absorbance level of crystal violet released from *C. procera* fibers and A_{panicp} is the absorbance level of crystal violet released from chemically modified fibers. A positive value results from the reduction in biofilm formation rate, due to the reduction in the amount of adhered species in the resulting material.

2.2 Methods

The morphology of the hollow tubes of *C. procera* and PANI-coated tubes was evaluated using scanning electron microscopy (SEM Vega 3XM Tescan) at an accelerating voltage of 20 kV. The structure of the material was scrutinized by the Fourier transform infrared (FTIR) spectrum with the measurement provided by an IR Prestige-21 FTIR spectrophotometer Shimadzu using the KBr technique. The X-ray diffraction (XRD) pattern was acquired using a DRX Miniflex Rigaku diffractometer. Absorbance spectra were measured using a Shimadzu–1650PC UV/visible spectrophotometer in the range of 300–800 nm (in 1 nm steps).

3 Results

3.1 Characterization of pristine and chemically modified fibers

3.1.1 Morphology

The SEM images shown in Fig. 2 were explored to evaluate different factors, such as the morphology of natural fibers and the influence of supports on overall polymerization.

As shown in Fig. 2a, b, small aggregates of PANI with an amorphous phase are observed for samples polymerized in the absence of tubular supports. From the images shown in Fig. 2c, d, it is possible to observe that *C. procera* are cylindrical and open-ended structures with a smooth surface and a diameter of 29.42 ± 2.50 µm in the absence of impurities on the fiber surface. The modification provided by PANI incorporation as a coating layer of fibers can be identified from the images in Fig. 2e, f. As can be seen, the irregular polymeric layer covers all of the fibers and introduces a granular aspect from PANI aggregates on the coated hollow fibers. Based on SEM images where the polymer layer was detached from the microtubes, it was possible to estimate the polymeric thickness as (1.29 ± 0.39) µm.

3.1.2 UV–Vis, FTIR, and XRD analyses

The extent of the conjugation, doping level, and nature of the synthesized PANI were elucidated from the measurements of the UV–Vis spectra for the as-prepared and undoped forms of PANI. As shown in Fig. 3, the as-prepared samples (doped PANI) present a polaron band (characteristic of PANI emeraldine salts) around 400 nm and a second broadband around 800 nm, which is associated with a small free-electron absorption tail [23]. On the other hand, the undoped form of PANI presents a band at 300–350 nm (associated with π–π^* transitions in the aromatic rings) and at 600 nm as a response of electronic transitions between quinoid and benzenoid species [23].

These results confirm the successful synthesis of emeraldine salt, the most appropriate species to be explored as an antibacterial coating layer. The FTIR spectra of PANI, *C. procera* and PANI-CP are shown in Fig. 4. The characteristics of both components are described by vertical lines in each spectrum. Relative to *C. procera*, as also reported in Ref. [17], characteristic peaks of the material are observed at 1737 cm^{-1} for acetal and uronic ester groups in hemicellulose, with hydrophobic behavior of fibers visualized from peak at 1640 cm^{-1}, C–O–C stretching vibrations of lignin at 1378 cm^{-1}, and C–O stretching vibration at 1108 and 1050 cm^{-1}.

The presence of PANI was confirmed from the FTIR spectrum of PANI-CP and PANI samples as follows: The signature of quinoid and benzenoid rings of PANI is present in peaks at 1570 and 1490 cm^{-1}. The stretching mode of the benzenoid ring is detected by peaks at 1299 and 1244 cm^{-1}, while the out-of-plane bending of C–H was observed at 828 cm^{-1}, as previously reported by [29]. In addition, bending vibrations of chloride ions (doping level of PANI chains) have been observed at 503 cm^{-1} [23]. These peaks confirm the polymerization of PANI on *C. procera* in the doped form.

In terms of the XRD pattern for pristine *C. procera* fibers, a single broad and intense reflection was observed at 23.08°, attributed to the crystalline components (002) of hemicellulose and alpha-cellulose [30, 31]. For PANI-coated samples (PANI-CP), the superposition of the peak at 23.08°

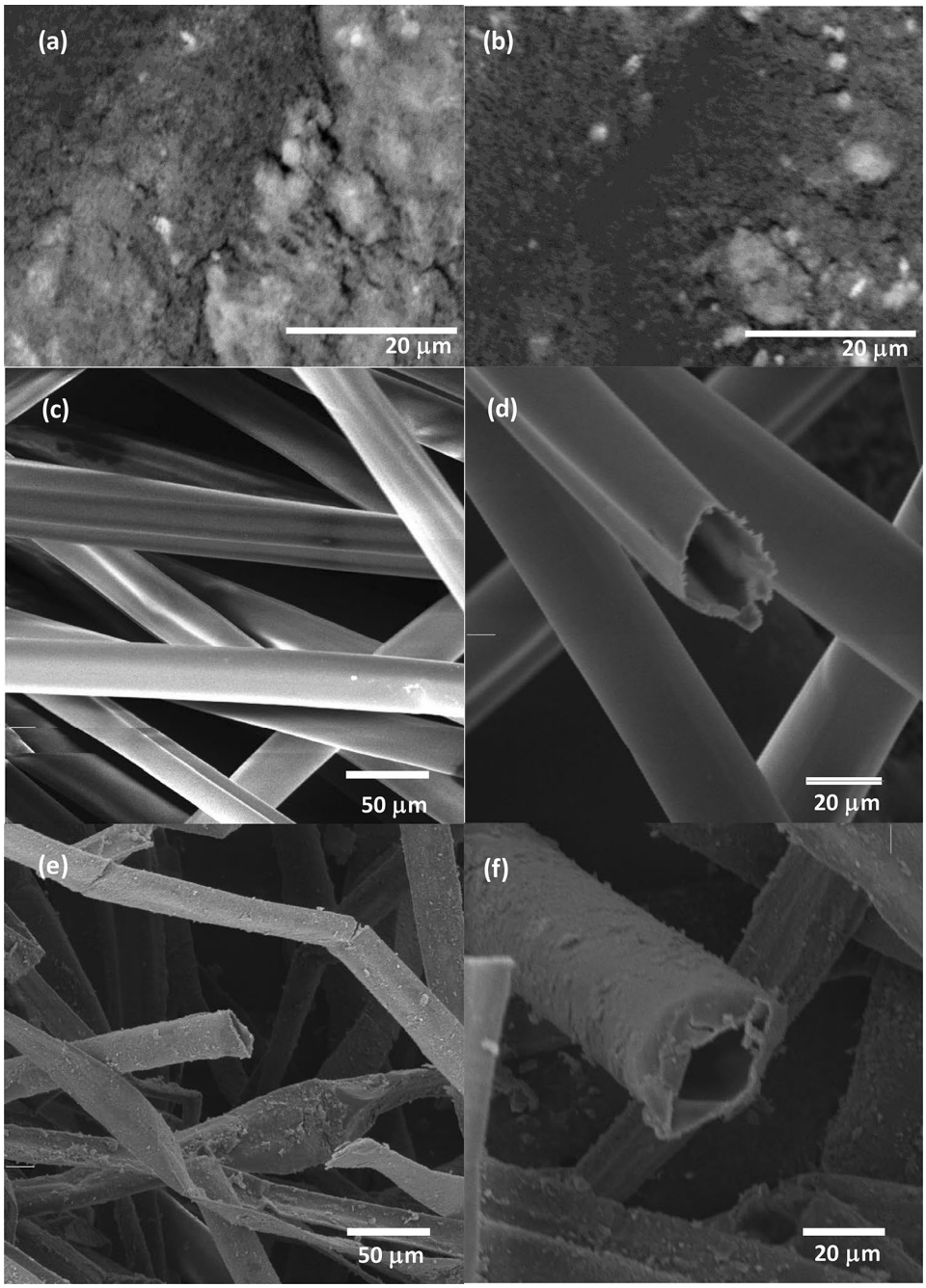

Fig. 2 SEM images of pure PANI (**a**, **b**), neat *C. procera* fibers (**c**, **d**) and PANI-CP fibers (**e**, **f**) at different magnifications

and a shoulder at 17.96°, which are associated with the (110) and (111) planes, are characteristic of the amorphous nature of PANI, which covers the *C. procera* fibers [29], as shown in Fig. 5. For pure PANI, the characteristic broad scattering reflection centers in the range of 20°–30° are confirmed by the curve in green [23].

3.2 Antibacterial activity of pristine and chemically modified fibers

The inhibition zone methodology was preliminarily applied to qualitatively evaluate the degree of antibacterial activity of pristine and chemically modified

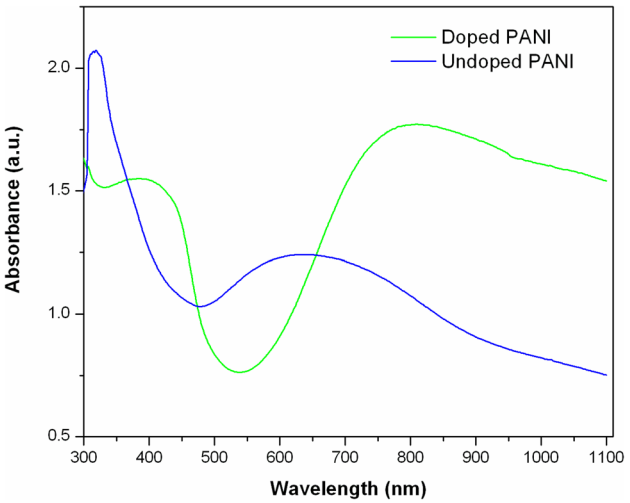

Fig. 3 UV–Vis spectra for blue PANI (undoped PANI) and green PANI (emeraldine salt form-doped PANI)

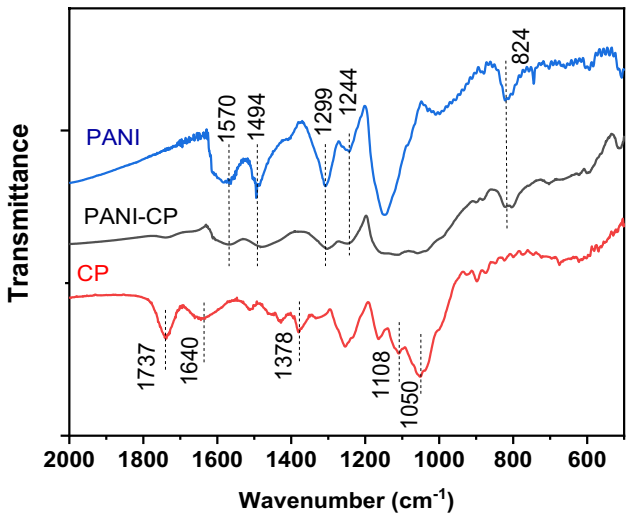

Fig. 4 FTIR spectrum of *C. procera* (CP), pure PANI (PANI) and PANI-CP

fibers against *S. aureus* and *E. coli*. These results can be explored as an indication of diffusive components and their potential as antibacterial agents. For this, colonies of *E. coli* (Fig. 6a, c) and *S. aureus* (Fig. 6b, d) were dispersed in agar plates in the presence of 6 disks. Two disks comprised a control sample containing pristine *C. procera*, 2 disks of PANI-coated fibers (PANI-CP), and 2 disks of pure PANI. As shown in Fig. 6, the comparison of inhibition haloes for different colonies revealed that, in both cases (against *E. coli* and *S. aureus*), the *C. procera* disk returned negligible inhibitory activity, while PANI-coated fibers and pure PANI showed a clear inhibitory figure against both *E. coli* (inhibition halo of 20 and 23 mm, respectively) and *S. aureus* (inhibition halo of 24 and 25 mm, respectively), confirming the improved diffusion on agar is observed for the PANI-CP sample against *S. aureus*.

These data confirm the antibacterial activity of doped PANI (emeraldine salt) [2], and the high inhibition halo values suggest that the release of diffusion species can cause potential disruption of the cell wall, favoring the antibacterial activity of the resulting material. By comparison with PANI-CP samples, a slight variation has been observed for the inhibition halos measured for pure PANI (24 and 25 mm, respectively). The best performance for PANI can be considered as a consequence of a higher density of active antibacterial material in resulting pellets of pure (and bulky) material, while PANI-CP is finely coated of CP microtubes with clear economic advantage for large-scale implementation. As expected, no antibacterial activity was observed for the CP sample.

To quantify the antibacterial activity of the resulting material, kill time assays were evaluated, not only to identify the antibacterial potential but also to determine the kinetics of action of the composites. For ease of comparison, the uncountable number of cells was 10^6 CFU. The results, shown in Fig. 7a, b, represent the counting of remaining viable cells after a fixed time of treatment. In agreement with data from the inhibition halo, negligible inhibition was observed for control samples (fibers of pristine *C. procera*), in that uncountable cells were observed for all intervals of time of treatment.

By contrast, the action of PANI-coated fiber (PANI-CP) on both colonies (*S. aureus* and *E. coli*) resulted in a progressive reduction in the viable cell count, reaching a complete inhibition (100% in bacterial counting) after 4 h of contact with *E. coli* and 3 h of contact with *S. aureus*.

The superior performance of conducting polymers (such as polypyrrole and PANI) against *S. aureus* has been previously reported [2–4, 32].

The observed activity of the PANI-CP composites confirms that different antibacterial mechanisms contribute to the overall response, described as follows:

- The available surface area of the materials (coating layer of PANI on *C. procera*) introduces advantages on bulky PANI (without support) because of the available sites for electrostatic interaction with bacterial cells.
- The electrostatic interaction takes place from the positively charged surface of PANI, which attracts the negatively charged bacterial surface, reinforcing the antibacterial mechanisms of PANI.
- The main mechanism is centered on the production of hydrogen peroxidase, which favors the production of reactive oxygen species that induce cell damage, leading to cellular death [22].

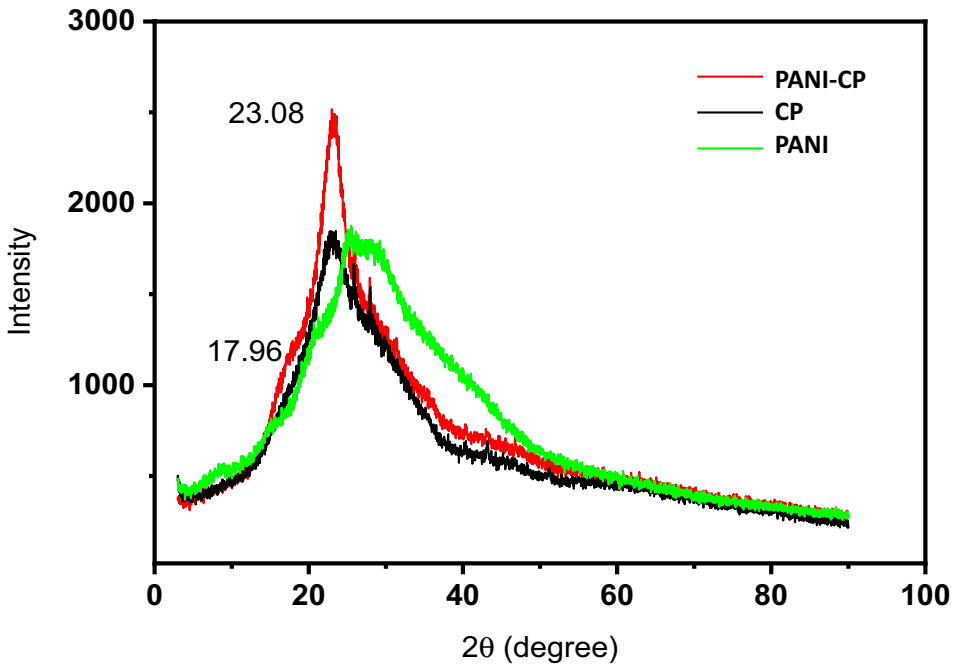

Fig. 5 XRD pattern of *C. procera* (CP), pure PANI (PANI) and PANI-CP

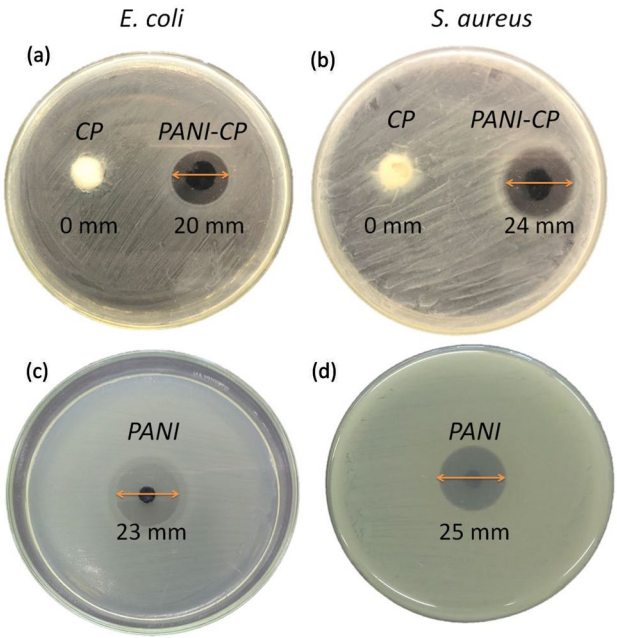

Fig. 6 Inhibition zones for disks of *C. procera* and PANI-CP against *E. coli* (**a**), *S. aureus* (**b**) and corresponding halos for pure PANI against *E. coli* (**c**) and *S. aureus* (**d**)

- The high conductivity degree of doped PANI perturbs the flow of electrons through electron transport chains in bacterial cells, favoring side effects due to the interaction with oxygen [22].

Another important aspect to be considered regarding these modified fibers is their ability to reduce the degree of biofilm formation. To evaluate this property, the amount of attached biofilm of *S. aureus* and *E. coli* in a control experiment was compared with active samples. In this case, we compared the amount of adsorbed biofilm on pristine *C. procera* fibers with corresponding PANI-coated samples. The absorbance level has been considered as a direct estimate of adhered biofilm on the fibers' surface. From the results summarized in Table 1, it is possible to identify a reasonable reduction in biofilm formation (39.96% reduction of *S. aureus*) as a consequence of surface modification induced by PANI deposition. Negligible variation was observed for biofilm adhesion of *E. coli*, characterizing a high degree of the coating by microorganisms on the resulting fibers. Corresponding assays for pure PANI are reported in Ref. [2].

These results confirm that the electrostatic and antibacterial activity of PANI-CP is more effective with the Gram-positive species. Despite the thicker peptidoglycan layer of these species, the stronger antibacterial activity of the resulting composite (revealed from faster kinetics in the kill time assays as illustrated in Fig. 7) inhibits *S. aureus*-based biofilm formation.

4 Conclusion

The development of low-cost and efficient antibacterial agents is favored by the strong antibacterial activity of PANI-CP fibers against both Gram-negative and

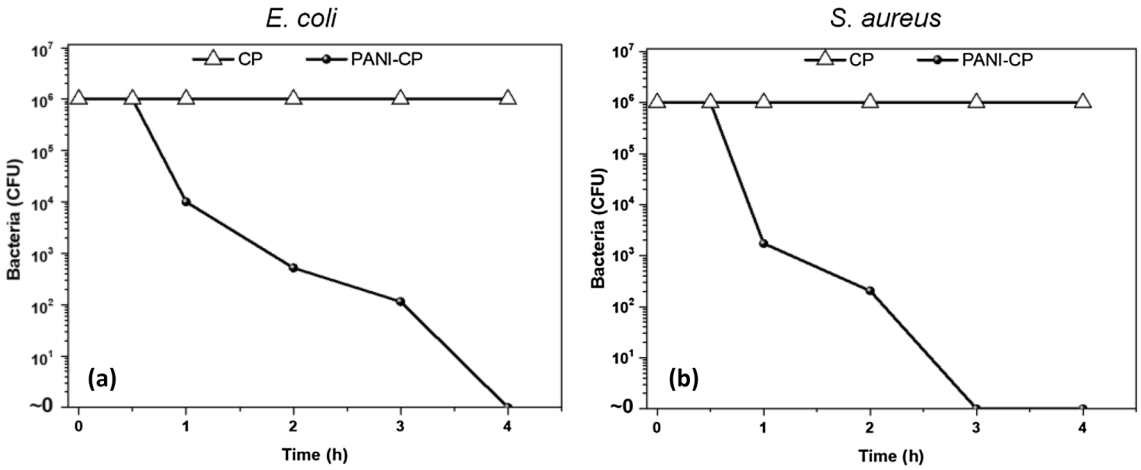

Fig. 7 Remaining CFU of **a** *E. coli* and **b** *S. aureus* treated with control samples of *C. procera* (CP) and PANI-CP fibers

Table 1 Absorbances (measured at 570 nm) and percentage of biofilm inhibition induced by chemical modification on fibers

Bacteria	Abs CP (570 nm)	Abs PANI-CP (570 nm)	%BI
S. aureus	2.046	1.229	39.96
E. coli	3.000	2.952	1.60

Gram-positive species (*E. coli* and *S. aureus*, respectively). The ease of preparation of coated and flexible hollow microtubes offers advantages relative to the production of reactive oxygen species and available electrons by conductive PANI in association with a high degree of (electrostatic) attraction of microorganisms in the direction of the surface of the fibers. The strong antibacterial activity against *S. aureus* is reinforced by inhibition of biofilm formation on modified fibers, which represents an important aspect concerning the inhibition of bacterial growth on treated surfaces.

Compliance with ethical standards

Conflict of interest The authors declare that they have no conflict of interest.

References

1. Alanis AJ (2005) Resistance to antibiotics: are we in the post-antibiotic era? Arch Med Res 36:697–705. https://doi.org/10.1016/j.arcmed.2005.06.009
2. dos Santos MR, Alcaraz-Espinoza JJ, da Costa MM, de Oliveira HP (2018) Usnic acid-loaded polyaniline/polyurethane foam wound dressing: preparation and bactericidal activity. Mater Sci Eng C 89:33–40. https://doi.org/10.1016/j.msec.2018.03.019
3. Lima RM, Alcaraz-Espinoza JJ, da Silva Jr FA, de Oliveira HP (2018) Multifunctional wearable electronic textiles using cotton fibers with polypyrrole and carbon nanotubes. ACS Appl Mater Interfaces 10:13783–13795. https://doi.org/10.1021/acsami.8b04695
4. da Silva Jr FA, de Araújo CM, Alcaraz-Espinoza JJ, de Oliveira HP (2018) Toward flexible and antibacterial piezoresistive porous devices for wound dressing and motion detectors. J Polym Sci Part B 56:1063–1072. https://doi.org/10.1002/polb.24626
5. Radwan AM, Alghamdi HA, Kenawy SK (2019) Effect of *Calotropisprocera* L. plant extract on seeds germination and the growth of microorganisms. Ann Agric Sci 64:183–187. https://doi.org/10.1016/j.aoas.2019.12.001
6. Shamim SA, Fatima L (2019) Pharmacological actions and therapeutic uses of Aak (*Calotropis procera*): a review. Pharm Innov J 8(2):40–47
7. Kumar V, Basu N (1994) Anti-inflammatory activity of the latex of *Calotropis procera*. J Ethnopharmacol 44:123–125. https://doi.org/10.1016/0378-8741(94)90078-7
8. Mascolo N, Sharma R, Jain S, Capasso F (1988) Ethnopharmacology of *Calotropis procera* flowers. J Ethnopharmacol 22:211–221. https://doi.org/10.1016/0378-8741(88)90129-8
9. Bilal H, Ali I, Uddin S, Khan I, Said A, Rahman MU, Khan AM, Shah AB, Ali A (2020) Biological evaluation of antimicrobial activity of *Calotropis procera* against a range of bacteria. J Pharmacogn Phytochem 9:31–35
10. Alzahrani HS, Mutwakil M, Sabir J, Saini KS, Alarif WM, Rizgallah MR (2017) Anticancer and antibacterial activity of *Calotropis procera* leaf extract. J Basic Appl Sci Res 7(12):18–25
11. Mohamed NH, Ismail MA, Abdel-Mageed WM, Shoreit AAM (2019) Antimicrobial activity of green silver nanoparticles from endophytic fungi isolated from *Calotropis procera* (Ait) latex. Microbiology 165:967–975. https://doi.org/10.1099/mic.0.000832
12. Akindele P, Fatunla O, Ibrahim K, Afolayan C (2017) Antibacterial and phytochemical screening of *Calotropis procera* leaf extracts against vancomycin and methicillin resistant bacteria isolated from wound samples in hospital patients. J Complement Altern Med Res 2(1):1–14. https://doi.org/10.9734/JOCAMR/2017/30975

13. Kumar S, Dewan S, Sangraula H, Kumar V (2001) Anti-diarrhoeal activity of the latex of *Calotropis procera*. J Ethnopharmacol 76(1):115–118. https://doi.org/10.1016/S0378-8741(01)00219-7
14. Pattnaik PK, Kar D, Chattoi H, Shahbazi S, Ghosh G, Kuanar A (2017) Chemometric profile and antimicrobial activities of leaf extract of *Calotropis procera* and *Calotropis gigantea*. Nat Prod Res 31(16):1954–1957. https://doi.org/10.1080/14786419.2016.1266349
15. Duan W, Xiao W, Wang N, Niu B, Zheng Y (2019) Removal of three fluoroquinolone antibiotics by $NaClO_2$-modified biosorbent from fruit fiber of *C. Procera*. J Nat Fibers 16:1–11. https://doi.org/10.1080/15440478.2019.1584080
16. Tu L, Duan W, Xiao W, Fu C, Wang A, Zheng Y (2018) *Calotropis gigantea* fiber derived carbon fiber enables fast and efficient absorption of oils and organic solvents. Sep Purif Technol 192:30–35. https://doi.org/10.1016/j.seppur.2017.10.005
17. Yoganandam K, Ganeshan P, NagarajaGanesh B, Raja K (2019) Characterization studies on *Calotropis procera* fibers and their performance as reinforcements in epoxy matrix. J Nat Fibers 16:1–13. https://doi.org/10.1080/15440478.2019.1588831
18. Nanlin S, Xuemei G, Hemin J, Jun G, Chao S, Ke T (2009) Antibacterial effect of the conducting polyaniline. J Mater Sci Technol 22:289–290
19. Tamboli MS, Kulkarni MV, Patil RH, Gade WN, Navale SC, Kale BB (2012) Nanowires of silver–polyaniline nanocomposite synthesized via in situ polymerization and its novel functionality as an antibacterial agent. Colloids Surf B Biointerfaces 92:35–41. https://doi.org/10.1016/j.colsurfb.2011.11.006
20. Boomi P, Prabu HG, Mathiyarasu J (2013) Synthesis and characterization of polyaniline/Ag–Pt nanocomposite for improved antibacterial activity. Colloids Surf B Biointerfaces 103:9–14. https://doi.org/10.1016/j.colsurfb.2012.10.044
21. Boomi P, Prabu HG (2013) Synthesis, characterization and antibacterial analysis of polyaniline/Au–Pd nanocomposite. Colloids Surf A Physicochem Eng Asp 429:51–59. https://doi.org/10.1016/j.colsurfa.2013.03.053
22. Robertson J, Gizdavic-Nikolaidis M, Nieuwoudt MK, Swift S (2018) The antimicrobial action of polyaniline involves production of oxidative stress while functionalisation of polyaniline introduces additional mechanisms. PeerJ 6:e5135. https://doi.org/10.7717/peerj.5135
23. Dhivya C, Vandarkuzhali SAA, Radha N (2016) Antimicrobial activities of nanostructured polyanilines doped with aromatic nitro compounds. Arab J Chem 12(8):3785–3798. https://doi.org/10.1016/j.arabjc.2015.12.005
24. Kucekova Z, Kasparkova V, Humpolicek P, Sevcikova P, Stejskal J (2013) Antibacterial properties of polyaniline-silver films. Chem Pap 67:1103–1108. https://doi.org/10.2478/s11696-013-0385-x
25. Liang X, Sun M, Li L, Qiao R, Chen K, Xiao Q, Xu F (2012) Preparation and antibacterial activities of polyaniline/$Cu_{0.05}Zn_{0.95}O$ nanocomposites. Dalton Trans 41:2804–2811. https://doi.org/10.1039/C2DT11823H
26. Cao E, Duan W, Wang F, Wang A, Zhegn Y (2017) Natural cellulose fiber derived hollow-tubular-oriented polydopamine: in-situ formation of Ag nanoparticles for reduction of 4-nitrophenol. Carbohydr Polym 158:44–50. https://doi.org/10.1016/carbpol.2016.12.004
27. Yang Q-Q, Gao L-F, Zhu Z-Y, Hu C-X, Huang Z-P, Liu R-T, Wang Q, Gao F, Zhang H-L (2018) Confinement effect of natural hollow fibers enhances flexible supercapacitor electrode performance. Electrochim Acta 260:204–211. https://doi.org/10.1016/j.electacta.2017.11.170
28. Pereira VR, Isloor AM, Bhat UK, Ismail A (2014) Preparation and antifouling properties of PVDF ultrafiltration membranes with polyaniline (PANI) nanofibers and hydrolysed PSMA (H-PSMA) as additives. Desalination 351:220–227. https://doi.org/10.1016/j.desal.2014.08.002
29. Hindi S (2013) *Calotropis procera*: the miracle shrub in the Arabian Peninsula. Int J Sci Eng Investig 2:48–57
30. Oun AA, Rhim J-W (2016) Characterization of nanocelluloses isolated from Ushar (*Calotropis procera*) seed fiber: effect of isolation method. Mater Lett 168:146–150. https://doi.org/10.1016/j.matlet.2016.01.052
31. da Silva Jr FA, Alcaraz-Espinoza JJ, da Costa MM, de Oliveira HP (2017) Synthesis and characterization of highly conductive polypyrrole-coated electrospun fibers as antibacterial agents. Compos Part B Eng 129:143–151. https://doi.org/10.1016/j.compositesb.2017.07.080
32. da Silva Jr FAG, Queiroz JC, Macedo ER, Fernandes AWC, Freire NB, da Costa MM, de Oliveira HP (2016) Antibacterial behavior of polypyrrole: the influence of morphology and additives incorporation. Mater Sci Eng C 62:317–322. https://doi.org/10.1016/j.msec.2016.01.067